Supplementary Materials for

Short Communication: Aging of basalt volcanic systems and decreasing CO_2 consumption by weathering

This supplementary material describes available information on volcanic basalt areas and calculation procedures. For the active volcanic fields (AVF) a detailed description of the calculation for the Holocene area fraction is given. Additionally, a description of the new alkalinity flux equation for young active basaltic areas and an explanation for the calculation of the global fluxes is provided.

Part One: Summary of data compilation

Table S1: Summary of the data of IVFs and AVFs used for this study.

No.	Name	Volcanic activity	T (°C)	Runoff (mm/a)	HCO_3^- (μmol/L)	Latitude	Longitude	Holocene fraction (%)	Reactivity
1	Massif Central	Inactive	8.7	406	916	45.77	2.96	0.00	1.02
2	South Africa	Inactive	12.7	244	1728	-25.28	29.63	0.00	0.87
3	Karelia	Inactive	-2.0	285	460	65.00	31.00	0.00	0.75
4	Coastal Deccan	Inactive	25.1	1690	657	16.93	73.51	0.00	0.98
5	Interior Deccan	Inactive	25.4	401	2839	21.00	74.00	0.00	0.98
6	Siberia Traps	Inactive	-8.5	254	501	65.00	100.00	0.00	1.14
7	E'Mei	Inactive	6.2	1350	238	27.45	103.33	0.00	1.04
8	Lei-Qiong	Inactive	24.0	797	1923	20.46	110.18	0.00	1.46
9	Nanjing	Inactive	15.2	330	1595	32.74	118.39	0.00	0.92
10	Xiaoxinganling	Inactive	-1.0	243	1065	49.09	128.17	0.00	1.39
11	Tumen River	Inactive	-4.0	273	763	42.50	128.50	0.00	1.37
12	Mudan River	Inactive	3.2	209	977	43.75	128.72	0.00	0.82
13	SE Australia	Inactive	13.0	74	5956	-38.19	142.86	0.00	0.90
14	Tasmania	Inactive	10.1	221	1704	-42.19	146.76	0.00	0.94
15	North Island, NZ	Inactive	13.0	920	478	-38.00	176.00	0.00	0.89
16	Kauai, Hawaii	Inactive	21.6	1747	588	22.00	-159.50	0.00	1.15
17	Columbia Plateau	Inactive	7.4	204	927	44.00	-118.50	0.00	0.57
18	NE America	Inactive	0.7	507	465	47.05	-75.32	0.00	1.12
19	Madeira Island	Inactive	13.5	1065	580	32.80	-17.00	0.00	1.21
20	Easter Island	Active	20.6	580	1306	-27.12	-109.37	3.36	0.91
21	Mt. Cameroon	Active	14.0	2120	2368	4.00	9.00	96.57	9.53
22	Mt. Etna	Active	14.9	640	9286	37.75	15.00	79.56	10.60
23	Virunga	Active	20.8	1709	2646	-1.50	29.50	48.02	5.36
24	La Réunion	Active	17.0	1712	1243	-21.12	55.54	28.13	3.28

25	Wudalianchi Lake	Active	-1.0	243	1919	48.70	126.14	14.82	2.50
26	Japan	Active	11.0	1236	584	35.92	135.36	8.70	1.69
27	Kamchatka	Active	-3.5	520	854	55.00	159.00	2.28	2.83
28	Taranaki	Active	10.0	1296	667	-39.30	174.00	8.00	2.16
29	Big Island, Hawaii	Active	15.4	935	951	19.50	-155.50	13.73	1.53
30	High Cascades	Active	6.8	382	776	45.19	-121.68	0.20	0.92
31	São Miguel	Active	16.0	879	2331	37.77	-25.50	9.35	3.38
32	Iceland	Active	0.7	1734	498	65.00	-18.00	13.19	4.11
33	Tianchi Lake	Active	-7.3	291	2445	42.00	128.05	65.34	5.90

In the following, all active volcanic provinces used for this study are described. Note, that for all inactive fields a detailed description of the input data can be found in Li et al. (2016), as well as the origin of the temperature, runoff and alkalinity concentration data for active volcanic fields. If watersheds are considered for the calculations of the Holocene area, they are based on the locations of the sampling points (see Li et al. (2016)).

In the following, the new data for active volcanic fields are described (Table S1)

Easter Island (No.20)

Easter Island is a volcanic island in the eastern pacific. Its volcanic nature is related to the Easter Island Hotspot. The geologic map used for this study was digitized after a map of Gioncada et al. (2010) and references therein. The island is composed mostly of hawaiites, mugearites and olivine basalts and it comprises volcanic ages from 3 Ma to recent. The different age classifications and lithologies are listed in the table below. Due to the precise age information the rocks could be directly classified into Holocene rocks and non-Holocene rocks. The total basaltic area of the island is 162.28 km^2, the Holocene area 5.45 km^2 and the non-Holocene area 156.82 km^2, resulting in a Holocene area fraction of 3.36%.

Table S2: Classification of the map data of Easter Island. The first three columns provide the original map data, whereas the column "System/Series" shows our interpretation of the map data.

Name	Description	Age	System/Series
TE1	Terevaka, hawaiites and olivine basalts	1.9-0.3 Ma	non-Holocene
TE2	Terevaka, hawaiites and olivine basalts	1.9-0.3 Ma	non-Holocene
TE3	Terevaka, hawaiites and olivine basalts	1.9-0.3 Ma	non-Holocene
HH2	Anakena, Hiva-Hiva, hawaiites and olivine basalts	0-2000a ago	Holocene
RA1	Rano Aroi, hawaiites, olivine basalts and mugearites	0.2 Ma	non-Holocene
RA5	Rano Aroi, hawaiites, olivine basalts and mugearites	0.2 Ma	non-Holocene
RA4	Rano Aroi, hawaiites, olivine basalts and mugearites	0.2 Ma	non-Holocene
RA2	Rano Aroi, hawaiites, olivine basalts and mugearites	0.2 Ma	non-Holocene
RA8	Rano Aroi, hawaiites, olivine basalts and mugearites	0.2 Ma	non-Holocene
RA7	Rano Aroi, hawaiites, olivine basalts and mugearites	0.2 Ma	non-Holocene
RA6	Rano Aroi, hawaiites, olivine basalts and mugearites	0.2 Ma	non-Holocene
RA3	Rano Aroi, hawaiites, olivine basalts and mugearites	0.2 Ma	non-Holocene
HH1	Anakena, Hiva-Hiva, hawaiites and olivine basalts	0-2000a ago	Holocene
PO2	Polke, alkali basalts, hawaiites to mugearites	3-0.61 Ma	non-Holocene

PO1	Polke, alkali basalts, hawaiites to mugearites	3-0.61 Ma	non-Holocene
PO5	Polke, alkali basalts, hawaiites to mugearites	3-0.61 Ma	non-Holocene
PO4	Polke, alkali basalts, hawaiites to mugearites	3-0.61 Ma	non-Holocene
TR	Maunga Orito, rhyolite; Maunga Parehe, trachyte	not known	not considered
PO3	Polke, alkali basalts, hawaiites to mugearites	3-0.61 Ma	non-Holocene
RK1	Rano Kau, alkali basalts, hawaiites to benmoreites	2.5-0.2 Ma	non-Holocene
RK2	Rano Kau, alkali basalts, hawaiites to benmoreites	2.5-0.2 Ma	non-Holocene
TA4	Tangaroa, hawaiites, olivine basalts and mugearites	0.2 Ma	non-Holocene
TA1	Tangaroa, hawaiites, olivine basalts and mugearites	0.2 Ma	non-Holocene
TA2	Tangaroa, hawaiites, olivine basalts and mugearites	0.2 Ma	non-Holocene
TA6	Tangaroa, hawaiites, olivine basalts and mugearites	0.2 Ma	non-Holocene
TA3	Tangaroa, hawaiites, olivine basalts and mugearites	0.2 Ma	non-Holocene
TA5	Tangaroa, hawaiites, olivine basalts and mugearites	0.2 Ma	non-Holocene
TA7	Tangaroa, hawaiites, olivine basalts and mugearites	0.2 Ma	non-Holocene

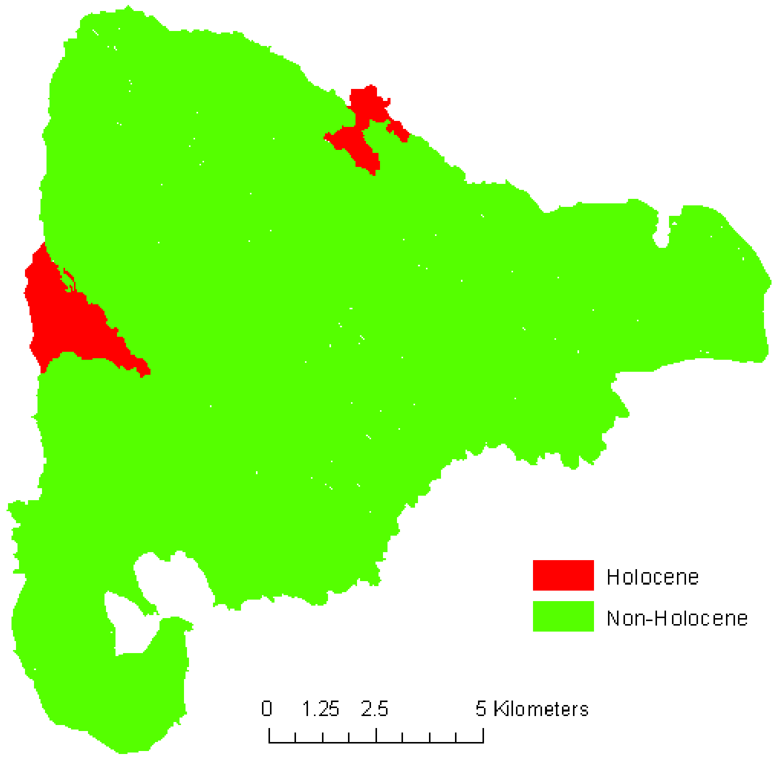

Figure S1: Map of Easter Island showing the Holocene and non-Holocene areas.

Table S3: Calculated areas for Easter Island.

Area Holocene (km^2)	**Area Non-Holocene (km^2)**	**Area Quaternary (km^2)**	**Total Area (km^2)**	**Holocene (%)**
5.45	156.83	0	162.28	3.36

Mount Cameroon (No.21)

Mount Cameroon is part of a volcanic chain at the coast of West Africa. The geological map was digitized from Le Maréchal (1975). The classification of the individual lithologies (see table below) results in a Holocene fraction of 96.57%.

Table S4: Classification of the lithologies of Mt. Cameroon. Note that the first three columns display the original map data, the column "System/Series" provides the authors interpretation.

Name	Description	Age	System/Series
beta1	Séries inférieures: basaltes parfois andésitiques sous forme de coulées et de dykes	Oligocene	non-Holocene
beta3	Séries supérieures: basaltes parfois andésitiques sous forme de coulées et cinérites	quatenaire récente	Holocene

Table S5: Area calculation of Mt. Cameroon.

Area Holocene (km^2)	Area non-Holocene (km^2)	Area Quaternary (km^2)	Total Area (km^2)	Holocene (%)
1112.63	39.48	0	1152.11	96.57

Figure S2: Map of Mount Cameroon showing the Holocene and non-Holocene area.

Mount Etna (No.22)

Mount Etna is located at a subduction zone in Italy. Its geological map was digitized from Branca et al. (2011). The detailed description of the lithologies can be seen below and provides a classification into Holocene, non-Holocene and Quaternary.

The Quaternary rocks are of an age of 15ka to 3.9ka, so that they have a time span of 11.1ka. Considering the Holocene time period going from 0 to 11.7 ka the amount of Holocene coverage can be calculated by:

Holocene fraction = (Area Holocene + (Area Quaternary x (7.8ka / 11.1ka))) / Total Area

resulting in a Holocene fraction area of 79.56%.

Table S6: Classification of Etna basaltic rocks showing the original map data (first four columns) and our interpretation of the data ("System/Series").

Symbol	Name	Description	Age	System/Series
26u	lava flows, cinder cones and bastions, and fall deposits	basaltic to benmoreitic	4ka - 122 b.C.	Holocene
27-1	Castings, cinder cones and bastions, and fall deposits	basaltic to mugearitica	122 b.C. - 1669	Holocene
27-2	Castings, cinder cones and bastions, and fall deposits	basaltic to mugearitica	1669-1971	Holocene
27-3	Lava flows, cinder cones and bastions, and fall deposits	basaltic to mugearitica	1971-current	Holocene
CB26u	Cono e bastione di scorie			Holocene
CB27-1	Cono e bastione di scorie			Holocene
CB27-2	Cono e bastione di scorie			Holocene
CB27-3	Cono e bastione di scorie			Holocene
10a	: intercalated flows in a powerful pyroclastic flow deposit	mugearitica	nn	non-Holocene
14	Succession of alternating flows in pyroclastic deposits	hawaiitica to mugearitica	nn	non-Holocene
15	flows intercalated with clastic deposits	mugearitica to benmoreitic	nn	non-Holocene
17	Casting interbedded with clastic deposits	benmoreite	nn	non-Holocene
18	flows	mugearitica - benmoreitic	nn	non-Holocene

18a	bodies subvulcanici materials come from lavas	mugearitica - benmoreitic	nn	non-Holocene
1a	bodies subvolcanici		nn	non-Holocene
21b	porfirichi flows	hawaiitica to mugearitica	nn	non-Holocene
22b	casting succession	hawaiitica	nn	non-Holocene
24	of breccia autoclastic often altered to hydrothermalism, associated with lava flows	benmoreitic	nn	non-Holocene
26b	deposit of debris avalanche monogenic, formed by lava mugearitica blocks	nn	nn	Quaternary
3b	massive lava flows	basaltic	nn	non-Holocene
1	underwater transitional composition of volcanics in tholeiitica consist of pillow lavas	tholeiitica	542.2-496.1ka	non-Holocene
10b	flows intercalated with breccias autoclastic and deposits epiclastici	hawaiitica to mugearitica	101.9ka	non-Holocene
11	Brecce autoclastic and deposits epiclastici	benmoreitic	107.2-99.1ka	non-Holocene
12	deposits associated with pyroclastic flows	mainly mugearitica	101.8-99.9ka	non-Holocene
13	castings and slag deposits	hawaiitica	93.0ka	non-Holocene
14a	subvulcanici bodies formed by lava massive	mugearitica	85.3ka	non-Holocene
16	: Casting intercalated with thin epiclastici deposits	mugearitica to benmoreitic	85.6ka	non-Holocene
19	Thin flows to the base, followed by a thick succession pyroclastic	mugeraitica	79.6-70.2ka	non-Holocene
2	lava flows	tholeiitica	332.4ka	non-Holocene
20	Fall and pyroclastic flow deposits	hawaiitica to benmoreitic	56.6-41.3ka	non-Holocene
21a	massive flows and autoclastic interbedded with breccia deposits	hawaiitica to mugearitica	29.1-32.5ka	non-Holocene
22	castings, scoria cones and fall deposits	hawaiitica to benmoreitic	28.7-42.1ka	non-Holocene
22	castings, scoria cones and fall deposits	hawaiitica to benmoreitic	28.7-42.1ka	non-Holocene

22	castings, scoria cones and fall deposits	hawaiitica to benmoreitic	28.7-42.1ka	non-Holocene
22	castings, scoria cones and fall deposits	hawaiitica to benmoreitic	28.7-42.1ka	non-Holocene
22	castings, scoria cones and fall deposits	hawaiitica to benmoreitic	28.7-42.1ka	non-Holocene
22	castings, scoria cones and fall deposits	hawaiitica to benmoreitic	28.7-42.1ka	non-Holocene
22	castings, scoria cones and fall deposits	hawaiitica to benmoreitic	28.7-42.1ka	non-Holocene
25b	reomorfiche flows	benmoreitic	15.4-15.0ka	non-Holocene
2a	subvolcanico body structure		320.0ka	non-Holocene
3a	strongly altered lava flows	basaltic	180.2ka	non-Holocene
4a	massive lava flows	basaltic to mugearitica	154.9-129.9ka	non-Holocene
4b	thin lava flows	basaltic to mugearitica	134.2ka	non-Holocene
6	Lave cataclasate	basaltic to mugearitica	128.7ka	non-Holocene
7	Succession Lava	mugearitica	126.4ka	non-Holocene
8	Succession lava with thin interbedded deposits epiclastici	hawaiitica to mugearitica	121.2-111.9ka	non-Holocene
9	lava flows interbedded with massive deposits of local epiclastici	hawaiitica to benmoreitic	105.8ka	non-Holocene
CB2	Cono e bastione di scorie			non-Holocene
CB22	Cono e bastione di scorie			non-Holocene
CB3a	Cono e bastione di scorie			non-Holocene
CB7	Cono e bastione di scorie			non-Holocene
26l	lava flows, cinder cones and bastions, and fall deposits	basaltic to benmoreitic	15ka - 4 ka	Quaternary
CB26l	Cono e bastione di scorie			Quaternary

Table S7: Table showing the calculated areas for Mount Etna.

Area Holocene (km^2)	Area non-Holocene (km^2)	Area Quaternary (km^2)	Total Area (km^2)	Holocene (%)
636.16	123.90	338.39	1098.46	79.56

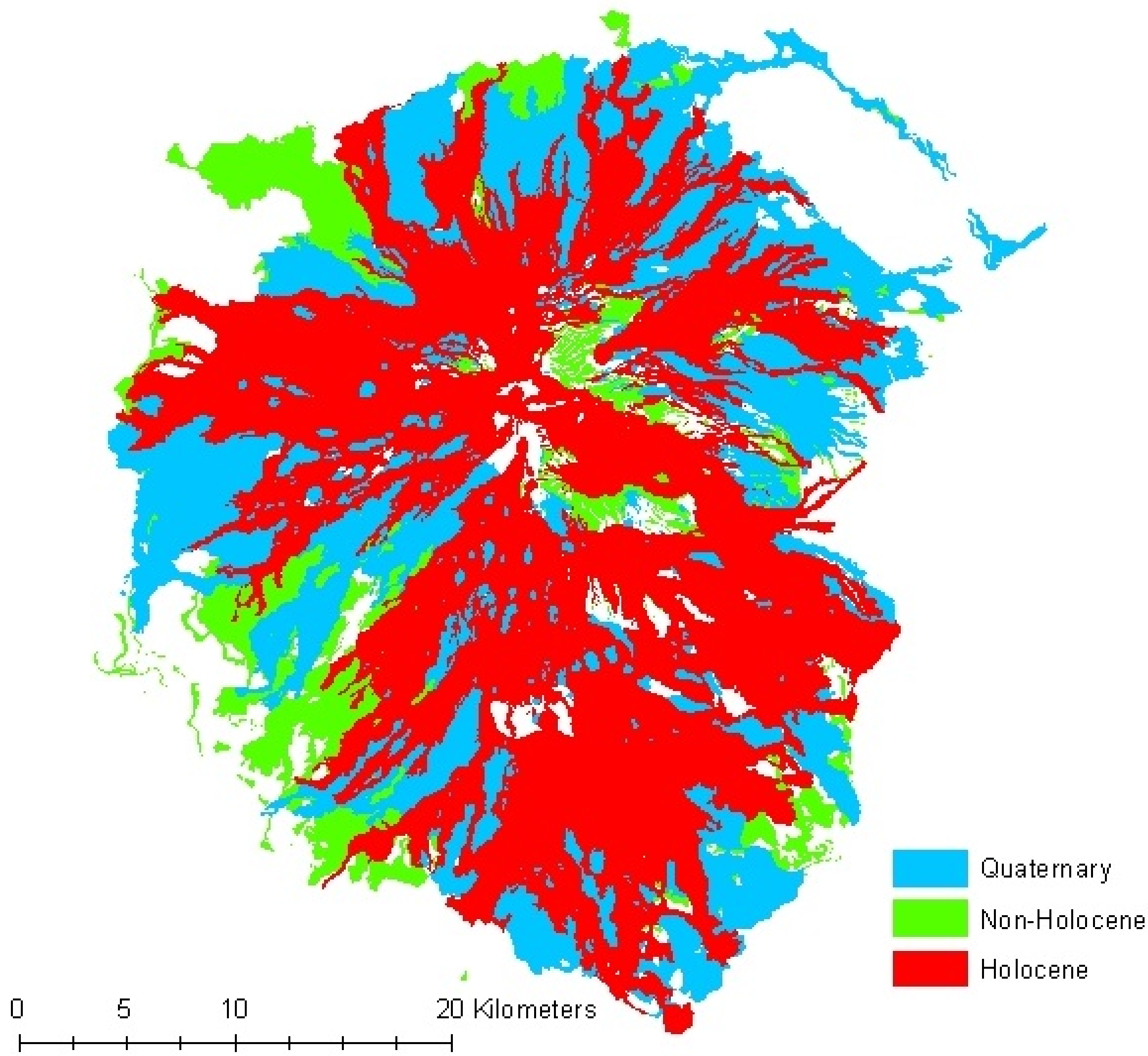

Figure S3: Map of Etna volcano showing the age distribution of basaltic rocks.

Virunga (No.23)

The Virunga Volcanic province is located in eastern central Africa and is related to the East African Rift system. The geologic map of this area was compiled out of four different maps from Smets et al. (2010), Balagizi et al. (2015), Petricec et al. (1971) and De Mulder et al. (1986).

The western part of the province is classified as purely Holocene, whereas the volcanic rocks become older to the east. Considering the Quaternary age period ranging from 0 to 2.58Ma, the Holocene percentage of the Quaternary area is calculated by the ratio of 11700a/2580000a. The total theoretical Holocene areal percentage is 48.02% using:

Holocene fraction = (Area Holocene + (Area Quaternary x (11700a / 2580000a))) / Total Area

Table S8: Classification of basaltic rocks in the Virunga province showing the individual volcanoes and our interpretation of their age.

Id	Volcano	System/Series
0	Nyiragongo	Holocene
1	Nyamuragira	Holocene
2	Muhabura	Pleistocene
3	Gahinga	Pleistocene
4	Muhabura-Gahinga	Pleistocene
5	Sabinyo	Pleistocene
6	Sabinyo-Gahinga	Pleistocene
7	Bisoke	Quaternary
8	Karisimbi	Quaternary
9	Remaining areas	Quaternary

Table S9: Calculated areas for Virunga province.

Area Holocene (km^2)	Area Non-Holocene (km^2)	Area Quaternary (km^2)	Total Area (km^2)	Holocene (%)
1518.62	320.69	1335.72	3175.03	48.02

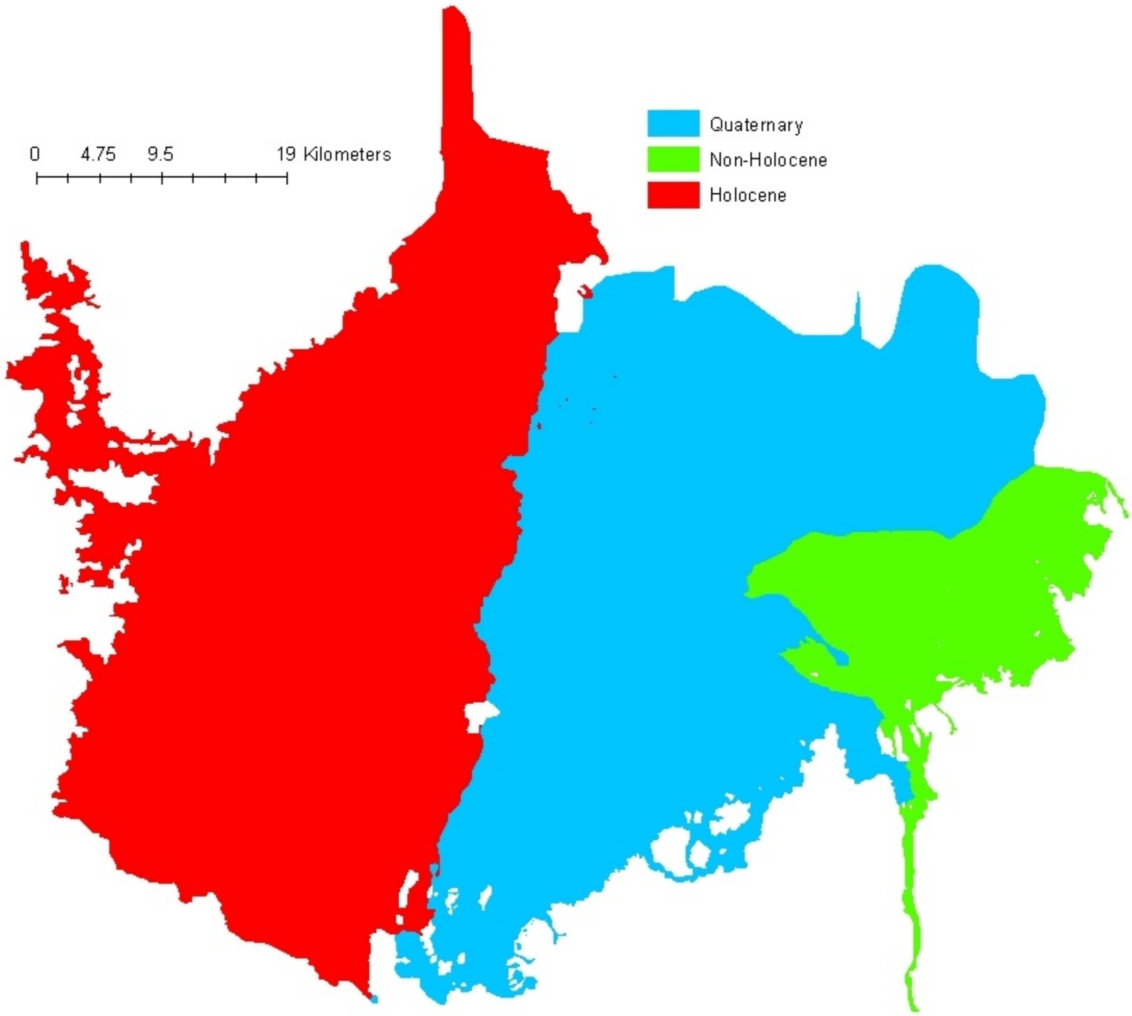

Figure S4: Map of the Virunga province showing the different areas of basalt classified after age.

La Réunion (No.24)

The volcanic island La Réunion belongs to a Hot Spot in the Indian Ocean and is comprised of Holocene, non-Holocene and Quaternary volcanic rocks. The geological map was digitized from Nehlig et al. (2006). The rocks can be divided into Holocene, non-Holocene and two different types of Quaternary rocks (Qu1, Qu2):

Qu1: <340ka → Holocene fraction = 11.7ka/340ka

Qu2: 65ka – 5ka → Holocene fraction = 6.7ka/60ka

Thus, the total Holocene fraction can be derived by:

$$\text{Holocene fraction} = (\text{Area Holocene} + (\text{Area Qu1} \times (11.7\text{ka} / 340\text{ka})) + (\text{Area Qu2} \times (6.7\text{ka} / 60\text{ka}))) / \text{Total Area}$$

providing a value of 28.13%.

Table S10: Classification of the basaltic rocks of La Réunion with the original data (first three columns) and our interpretation ("System/Series"). Note that "nn" represents that the age of the lithology is not known.

ID	Definition	Type	System/Series
beta 4	Coulées basaltiques	Massif du Piton de La Fournaise - Série du boucller ancien (450000 à 150000 ans)	non-Holocene
tfp	Pitons et projections	Massif du Piton de La Fournaise	nn
beta 7	Coulées basaltiques	Massif du Piton de La Fournaise - Série de la Plaine des Cafres (65000 à 5000 ans)	Quaternary2
beta 6	Coulées basaltiques	Massif du Piton de La Fournaise - Série Plaine des Sables (65000 à 5000 ans)	Quaternary2
beta 8	Coulées basaltiques	Massif du Piton de La Fournaise - Série volcanique subactuelle (<5000 ans)	Holocene
beta 5	Coulées basaltiques	Massif du Piton de La Fournaise - Série des Remparts (150000 à 65000 ans)	non-Holocene
beta 3	Coulées différencciées	Massif du Piton de La Fournaise - Série alcaline anté-Fournaise (530000 à 450000 ans)	non-Holocene
beta 8e	Coulées basaltiques dans l'Enclos	Massif du Piton de La Fournaise - Série volcanique subactuelle (<5000 ans)	Holocene
beta 1	Coulées basaltiques	Massif du Piton des Neiges - Série des océanites (>340000 ans)	non-Holocene

	à olivine		
beta 2	Coulées (basalte, hawaites, mugéarites)	Massif du Piton des Neiges - Série différenciée (<340000 ans)	Quaternary1
Br	Brèches d'avalanches de débris de Saint Gilles	Massif du Piton des Neiges - Série différenciée (<340000 ans)	Quaternary1
pc	Coulées ignimbritiques	Massif du Piton des Neiges - Série différenciée (<340000 ans)	Quaternary1
Tau	Coulées trachytiques du plateau de Belouve	Massif du Piton des Neiges - Série différenciée (<340000 ans)	Quaternary1

Table S11: Summary of calculated areas of La Réunion.

Area Holocene (km^2)	**Area non-Holocene (km^2)**	**Area Quaternary (km^2)**	**Total Area (km^2)**	**Holocene (%)**
208.11	270.98	359.60	838.68	28.13

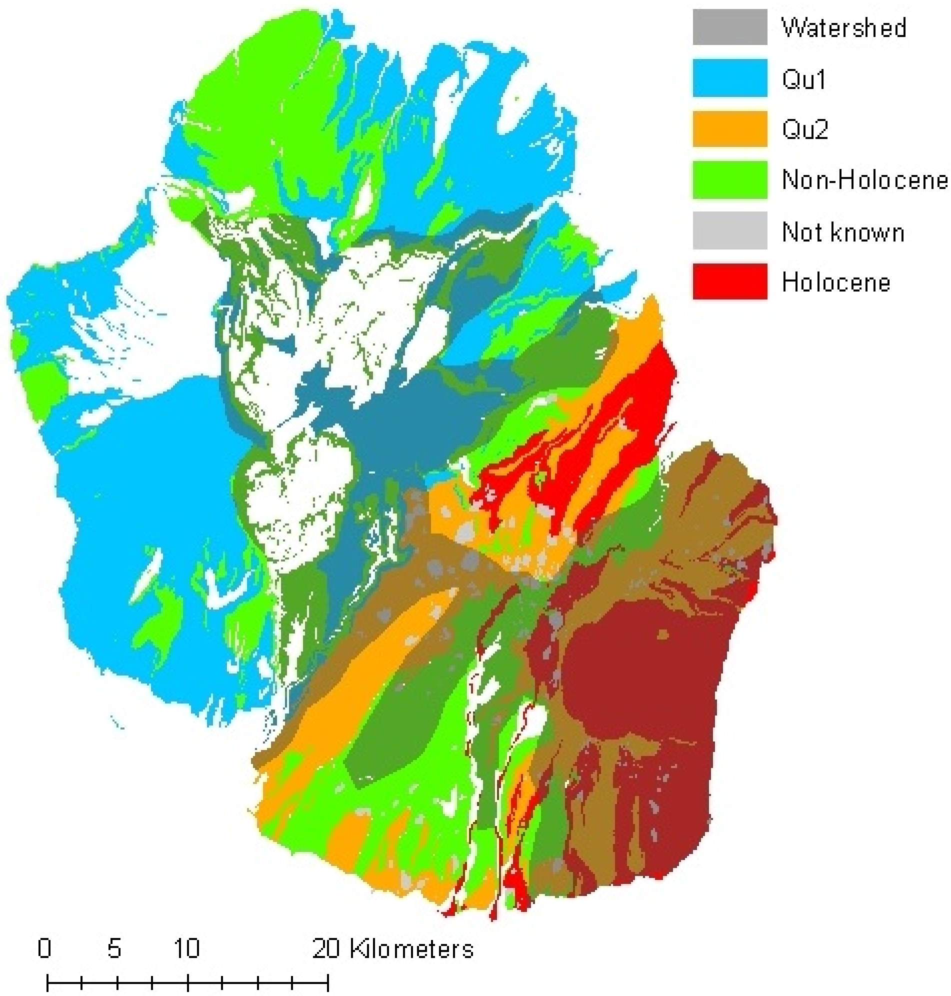

Figure S5: Map of La Réunion showing the basaltic ages and additionally the watershed of the water samples. Only the watershed area was considered for this study.

Wudalianchi Lake (No.25)

The basaltic rocks of Wudalianchi Lake are located in NE China and are of intraplate volcanic origin. The Geomap of Wudalianchi region was digitized after a map of the Ministry of Land and Resources of PRC, 2003 (unpublished work). The basalts can be separated into Holocene and non-Holocene and thus provide a calculated Holocene fraction of 14.82%.

Table S12: Classification of basalt of Wudalianchi Lake with the original map data (first three columns) and our interpretation shown in the column "System/Series".

Symbol	Litho	Age	System/Series
betaQ2w	basalt	middle pleistocene	non-Holocene
betaQ1j	basalt	lower pleistocene	non-Holocene
betaQ2b	basalt	middle pleistocene	non-Holocene
betaQ1g	basalt	tertiary	non-Holocene
betaQ42l	basalt	holocene	Holocene

Table S13: Calculated areas of Wudalianchi Lake.

Area Holocene (km^2)	Area non-Holocene (km^2)	Area Quaternary (km^2)	Total Area (km^2)	Holocene (%)
69.68	400.35	0	470.04	14.82

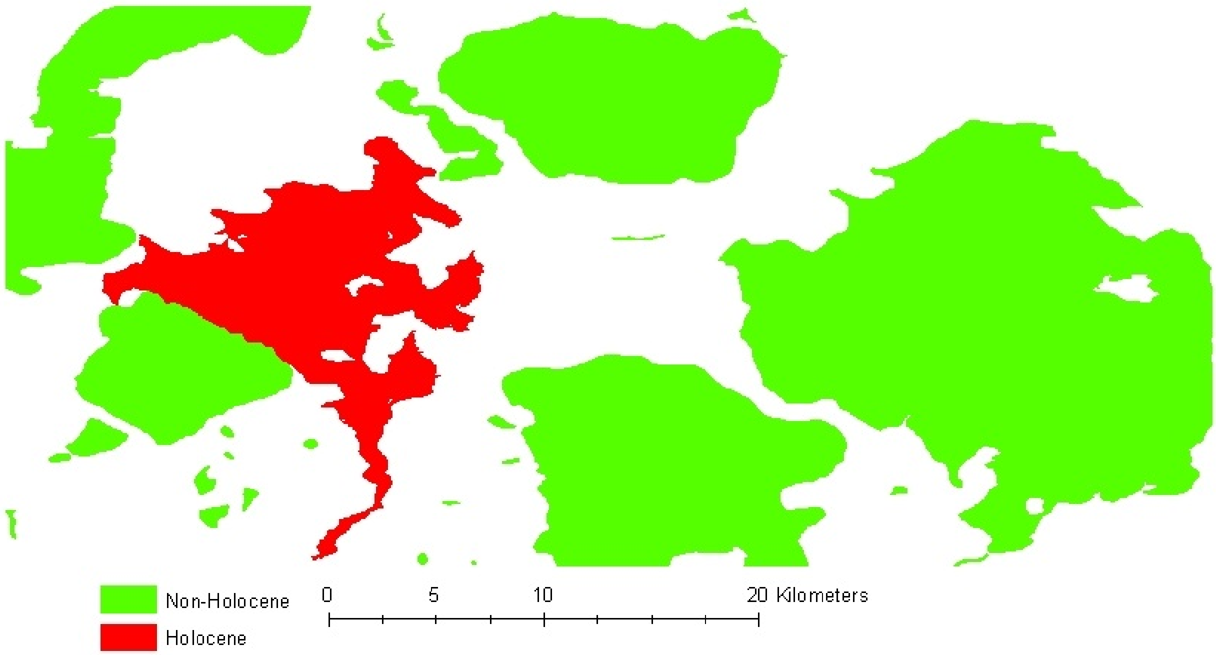

Figure S6: Map of Wudalianchi Lake showing the distribution of Holocene basaltic rocks.

Japan (No.26)

The geological data was derived of the Global Lithological Map (GLiM) by Hartmann and Moosdorf (2012) but only the watersheds of sample locations were used, thus the basaltic rocks can be divided into Holocene, non-Holocene and Quaternary rocks. The calculation procedure of the Holocene fraction of Quaternary rocks is the same as for the Virunga Province, and a final Holocene percentage of 8.70% is calculated.

Table S14: Classification of basaltic rocks for Japan after the GLiM (first three columns) and our interpretation "System/Series".

xx	Age_Min	Age_Max	System/Series
vb	Holocene	Holocene	Holocene
vb	Neogene	Neogene	non-Holocene
vb	Paleogene	Paleogene	non-Holocene
vb	Paleozoic	Proterozoic	non-Holocene
vb	Pleistocene	Pleistocene	non-Holocene
vb	Pliocene	Pliocene	non-Holocene
vb	Quaternary	Quaternary	Quaternary

Table S15: Calculated areas for Japan.

Area Holocene (km^2)	Area non-Holocene (km^2)	Area Quaternary (km^2)	Total Area (km^2)	Holocene (%)
243.30	2216.41	354.44	2814.15	8.70

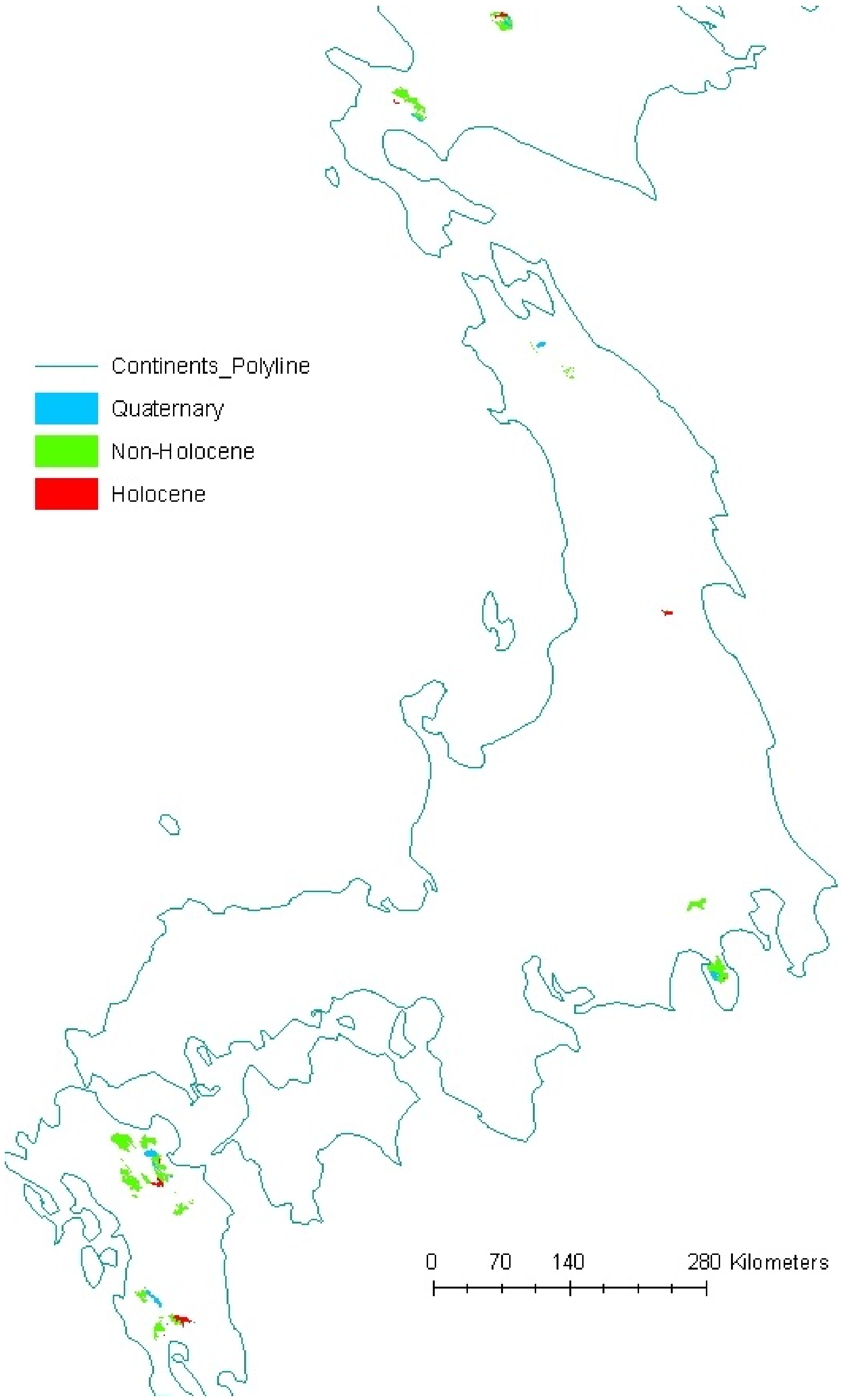

112

Figure S7: Map showing the watersheds and age classification of basaltic rocks for Japan.

113

Kamchatka (No.27)

The information of the basaltic rocks of the Kamchatka Peninsula is taken out of the GLiM (Hartmann and Moosdorf, 2012) and provides age information of Holocene, non-Holocene and Quaternary, where the Holocene fraction is again calculated as for the Virunga province. The Holocene fraction of the watershed of the Kamchatka Peninsula is 2.28%.

Table S16: Classification of basaltic rocks of the Kamchatka Peninsula after the GLiM (first three columns) and our interpretation ("System/Series").

Rock_Description	Age_Min	Age_Max	System/Series
Basalte, Andesite und deren Tuffe	Lower Quaternary	Lower Quaternary	non-Holocene
Basalte, Andesite und deren Tuffe	Middle Quarernary	Middle Quarernary	non-Holocene
volcanogenic formations, basic composition	Pliocene	Pliocene	non-Holocene
Basalte, Andesite und deren Tuffe	Quaternary	Quaternary	Quaternary
volcanogenic formations, basic composition	Upper Cretaceous	Upper Cretaceous	non-Holocene
Basalte, Andesite und deren Tuffe	Upper Quaternary	Middle Quarernary	Quaternary
Basalte, Andesite und deren Tuffe	Upper Quaternary	Upper Quaternary	Holocene

Table S17: Calculated areas of the Kamchatka Peninsula.

Area Holocene (km^2)	Area Non-Holocene (km^2)	Area Quaternary (km^2)	Total Area (km^2)	Holocene (%)
183.60	5588.34	2850.52	8622.46	2.28

123 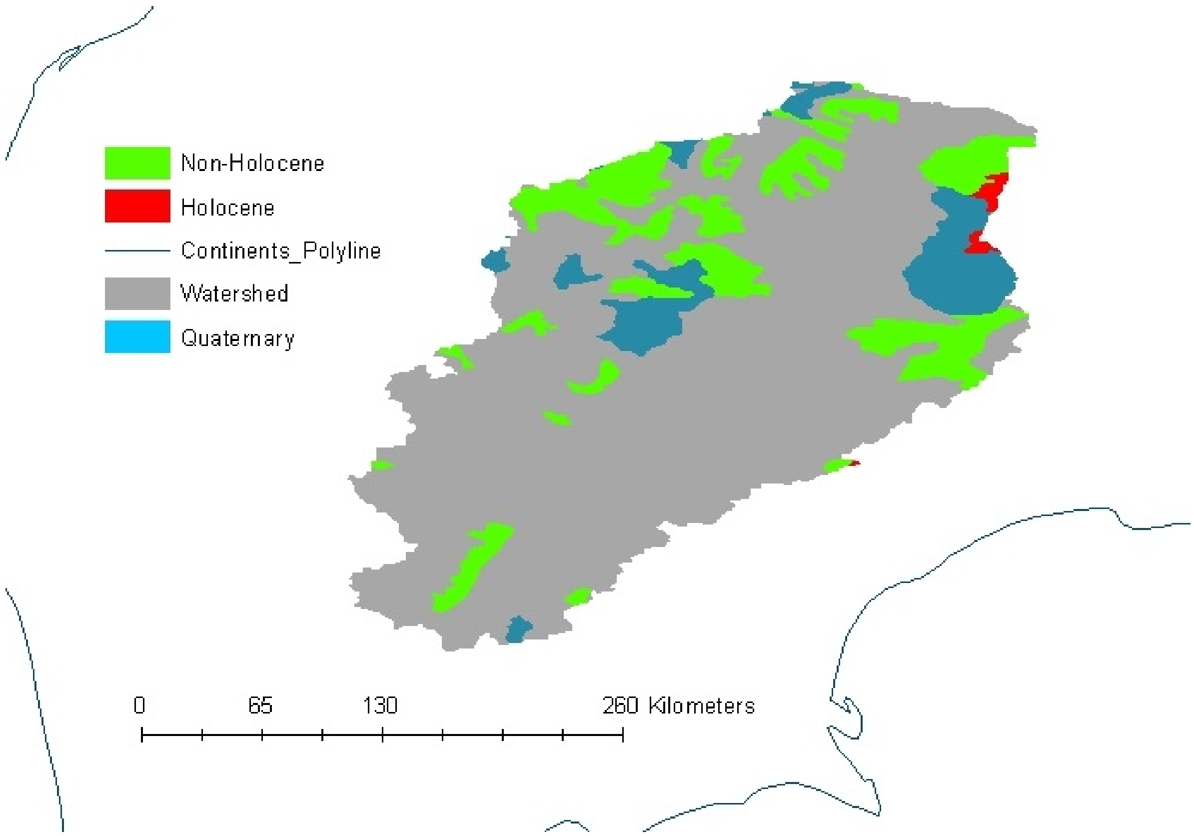

Figure S8: Map showing the watershed of the Kamchatka Peninsula.

124

125

Taranaki (No.28)

Taranaki volcano is located in the southern part of the Northern Island of New Zealand. Price et al. (1992) define four different regions of the Taranaki Volcanics (Paritutu, Kaitake, Pouakai and Egmont), where Mt. Egmont is the youngest. After Neall et al. (1986) the cone of Mt. Egmont represents about 8% of the total eruptive mass and is of an age of about 10ka (Holocene).

Big Island, Hawaii (No.29)

The geological map of the Big Island of Hawaii was digitized after an original map of Stearns and Macdonald (1946). Besides a separation into Holocene and non-Holocene rocks, two different types of Quaternary rocks exist:

Qu1: Hualalai Volcano: fraction Holocene = Area Qu1 x (11700a / 2580000a)

Qu2: Kilauea and Mauna Loa Volcano: fraction Holocene = Area Qu2 x (11700a / 126000a) with an assumption of “Latest Pleistocene” = Upper Pleistocene (0.126Ma).

In total, a Holocene fraction of 13.73% was calculated.

Table S18: Classification of the basaltic rocks of the Big Island of Hawaii after Stearns and Macdonald (1946) and our interpretation (“System/Series”).

Id	Volcano	Description	Age	System/Series
0	Kohala Mountain	Hawi Volcanic Series	Pleistocene	non-Holocene
1	Kohala Mountain	Pololu Volcanic Series	Pliocene and older	non-Holocene
2	Mauna Kea Volcano	Recent lavas	Holocene	Holocene
3	Mauna Kea Volcano	Pleistocene lavas	Pleistocene	non-Holocene
4	Mauna Kea Volcano	Hamakua Volcanic Series, capped by Pahala ash	Pleistocene	non-Holocene
5	Hualalai Volcano	Historic lavas	Holocene	Holocene
6	Hualalai Volcano	Prehistoric lavas	Quaternary	Quaternary1
7	Hualalai Volcano	Waawaa Volcanics (pumice cone, trachyte lava flow)	Pleistocene	non-Holocene
8	Kilauea Volcano	Historic lavas	Holocene	Holocene
9	Kilauea Volcano	Prehistoric lavas	Recent and latest Pleistocene	Quaternary2
10	Kilauea Volcano	Hilina Volcanic Series, capped by Pahala ash	Pleistocene	non-Holocene
11	Mauna Loa Volcano	Historic lavas	Holocene	Holocene
12	Mauna Loa Volcano	Prehistoric lavas	Recent and latest Pleistocene	Quaternary2
13	Mauna Loa Volcano	Kahuku Volcanic Series, capped by Pahala ash	Pleistocene	non-Holocene

14	Mauna Loa Volcano	Ninole Volcanic Series	Pliocene or older	non-Holocene

Table S19: Summary of the calculated areas for the Big Island of Hawaii.

Area Holocene (km^2)	**Area Non-Holocene (km^2)**	**Area Quaternary (km^2)**	**Total Area (km^2)**	**Holocene (%)**
929.17	3357.53	6252.29	10539.00	13.73

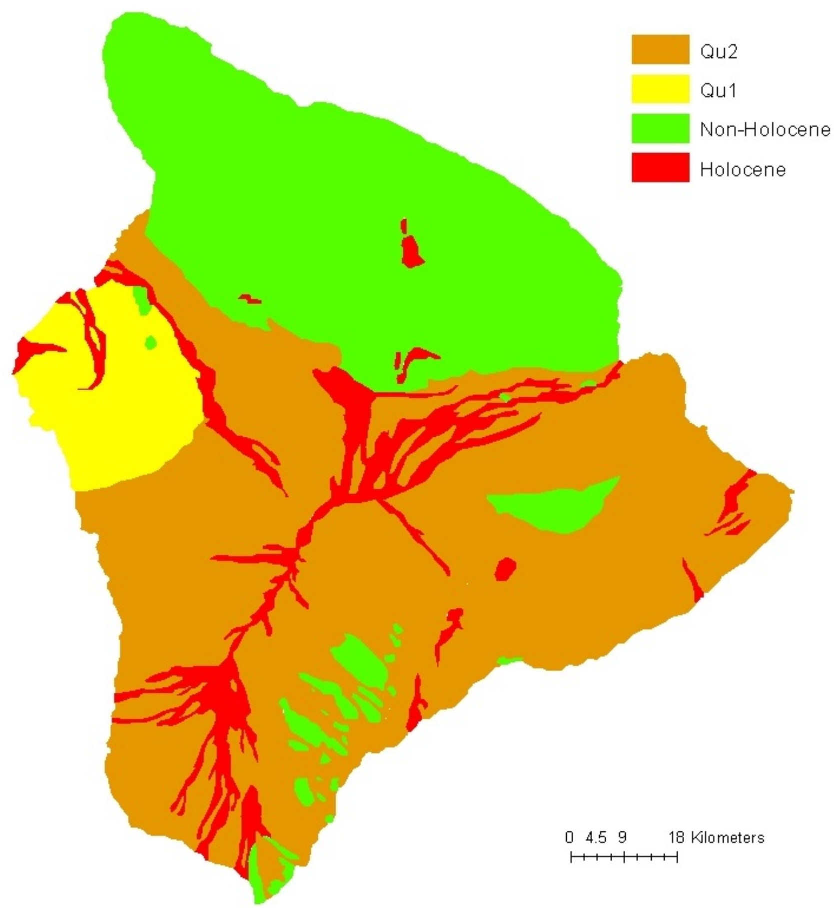

Figure S9: Map of the Big Island of Hawaii showing the different age distributions of basaltic rocks.

High Cascades (No.30)

The geological information for the High Cascades was derived of the GLiM by Hartmann and Moosdorf (2012) and results in a Holocene fraction of 0.20%.

Table S20: Classification of the basaltic rocks of the High Cascades Region after the Global Lithological Map (first three columns) and our interpretation ("System/Series").

Rock_Description	Age_Min	Age_Max	System/Series
basalt;	Early to Middle Miocene	Early to Middle Miocene	non-Holocene
tholeiite; siltstone	Eocene	Eocene	non-Holocene
basalt; andesite	Late Eocene to Oligocene	Late Eocene to Oligocene	non-Holocene
mafic volcanic rock;	Late Miocene to Pliocene	Late Miocene to Pliocene	non-Holocene
basalt; volcanic breccia (agglomerate)	Middle Eocene to Late Eocene	Middle Eocene to Late Eocene	non-Holocene
basalt (tholeiite); andesite	Middle Miocene	Middle Miocene	non-Holocene
basalt;	Middle Miocene	Middle Miocene	non-Holocene
andesite; basalt	Middle to Late Miocene	Middle to Late Miocene	non-Holocene
basalt; andesite	Miocene	Miocene	non-Holocene
basalt; rhyolite	Miocene-Pliocene	Miocene-Pliocene	non-Holocene
basalt; volcanic breccia (agglomerate)	Oligocene to Miocene	Oligocene to Miocene	non-Holocene
basalt; andesite	Pleistocene to Holocene	Pleistocene to Holocene	Quaternary
basalt; andesite	Pliocene to Pleistocene	Pliocene to Pleistocene	non-Holocene
andesite; basalt	Quaternary	Quaternary	Quaternary
andesite; basalt	Tertiary (2-24 Ma)	Tertiary (2-24 Ma)	non-Holocene
Andesite; basalt	Miocene	Miocene	non-Holocene

Table S21: Summarized area calculation for the watersheds of the High Cascades.

Area Holocene (km^2)	Area Non-Holocene (km^2)	Area Quaternary (km^2)	Total Area (km^2)	Holocene (%)
0	3033.92	2479.39	5513.31	0.20

150

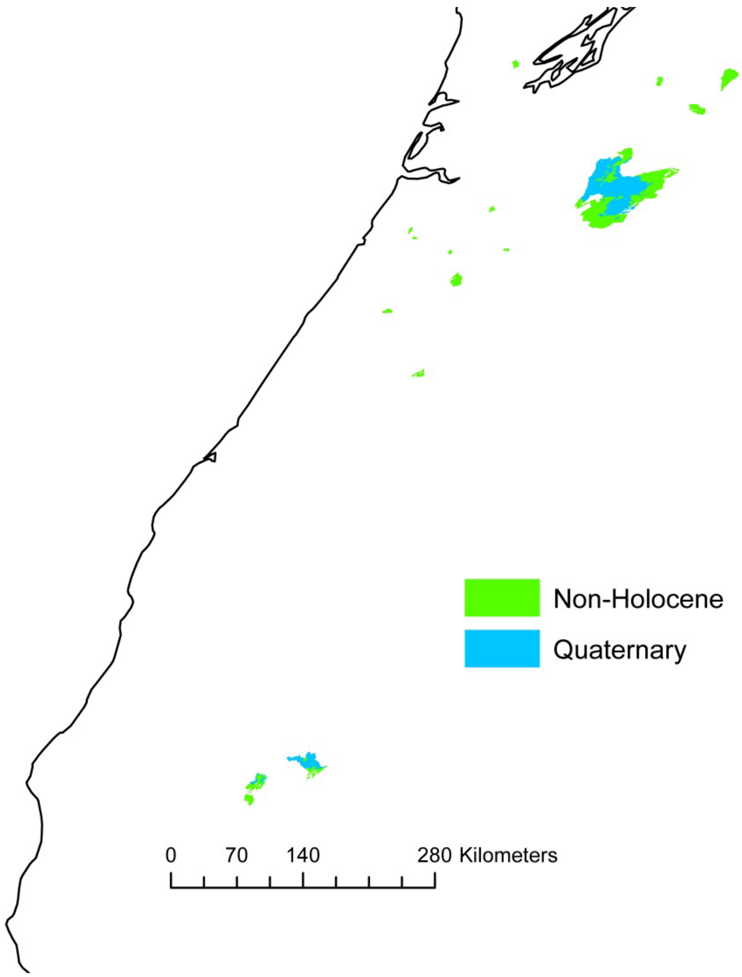

151

Figure S10: Map of the watersheds of the High Cascades.

152

Sao Miguel (No.31)

Sao Miguel is related to a Hot Spot in the northern Atlantic. The geological map was digitized after Moore (1990). There are only two watersheds considered in this study and the age of the basaltic rocks can be divided into two different Quaternary classes:

Qu1: fraction Holocene = Area Qu1 x (11700a / 200000a) (Agua de Pau Volcano, 0-200ka)

Qu2: fraction Holocene = Area Qu2 x (11700a / 100000a) (Furnas Volcano, 0-100ka)

Table S22: Classification of the basaltic rocks of Sao Miguel from the original data and our interpretation ("System/Series").

Id	Name	Type	Age	System/Series
2	Agua de Pau Volcano	trachyte stratovolcano	0-200ka	Quaternary1
4	Furnas Volcano	trachyte stratovolcano	0-100ka	Quaternary2

Table S23: Summary of the calculated areas of the watersheds of Sao Miguel.

Area Holocene (km^2)	Area Non-Holocene (km^2)	Area Quaternary (km^2)	Total Area (km^2)	Holocene (%)
0	0	47.04	47.04	9.35

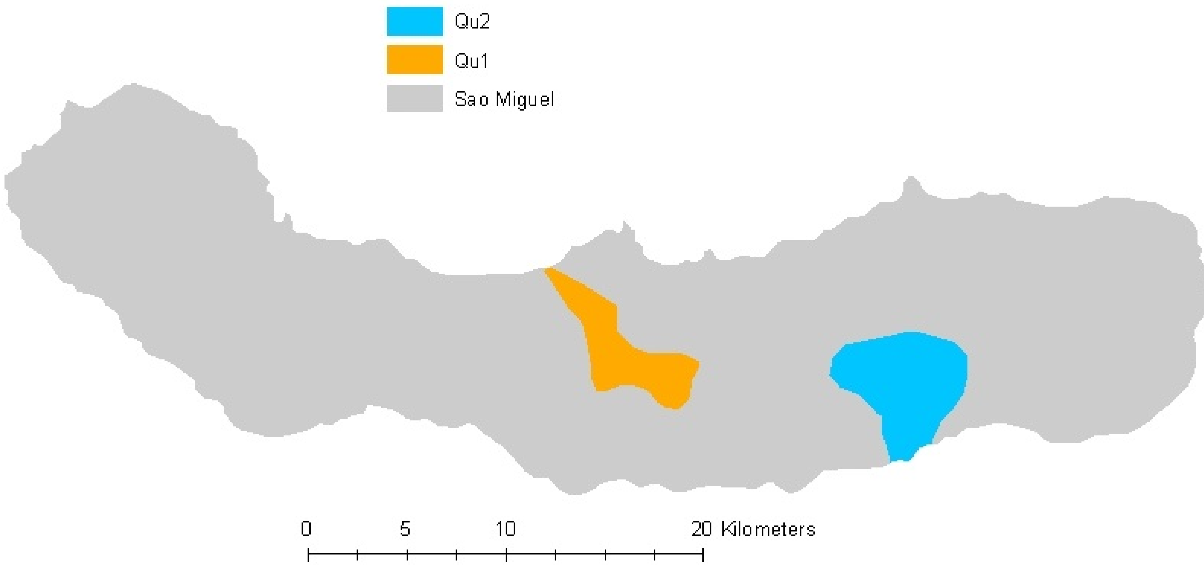

Figure S11: Map of Sao Miguel showing the two watersheds considered in this study.

Iceland (No.32)

The information of the basaltic rocks of Iceland are derived from the GLiM (Hartmann and Moosdorf, 2012) and can be classified into Holocene, non-Holocene and Quaternary (for the calculation see Virunga Province) and results in a Holocene coverage of 13.19%.

Table S24: Description of the basaltic rocks of Iceland after the GLiM (first three columns) and our interpretation ("System/Series").

Rock_Description	Age_Min	Age_Max	System/Series
Basalt and andesite	Holocene (postglacial time)	Holocene (postglacial time)	Holocene
Basic and intermediate hyaloclastites, lavas and associated sediments	Late Pleistocene	Late Pleistocene	non-Holocene
Basic and intermediate lavas and pyroclastic rocks (mainly hyaloclastite)	Late Pliocene, Early Pleistocene, 3.3 -	Late Pliocene, Early Pleistocene, 3.3 -	non-Holocene
Ocean-floor basalt; on land also intermediate volcanic rocks and sedimentary rocks	Miocene	Miocene	non-Holocene
Basic and intermediate volcanic rocks with intercalated sedimentary rocks	Miocene-Early Pliocene, older than 3.3 M	Miocene-Early Pliocene, older than 3.3 M	non-Holocene
Ocean-floor basalt	Pliocene	Pliocene	non-Holocene
Ocean-floor basalt	Quaternary	Quaternary	Quaternary

Table S25: Summary of the area calculation for Iceland.

Area Holocene (km^2)	Area Non-Holocene (km^2)	Area Quaternary (km^2)	Total Area (km^2)	Holocene (%)
13196.86	86773.61	104.36	100075.00	13.19

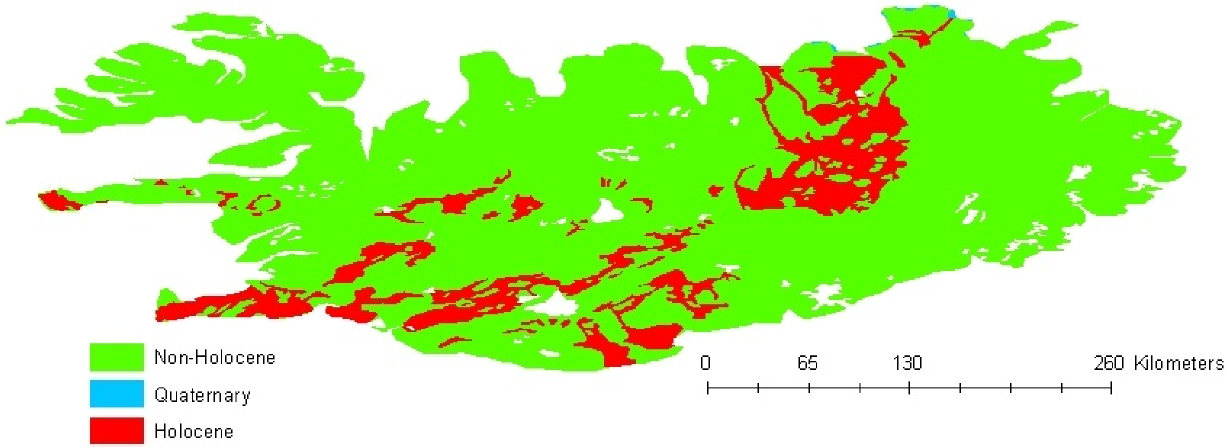

Figure S12: Map of Iceland showing the distribution of the age of basaltic rocks.

Tianchi Lake (No.33)

The geological map of the Tianchi Lake region was derived by Paone and Yun (2016). The basalts can be directly separated into Holocene and non-Holocene age. The total basaltic area is 11.31 km² and a Holocene fraction area of 65.34% can be calculated. The value for the runoff was calculated from Fekete et al. (2002).

Table S26: Description of the basaltic rocks of Tianchi Lake after Paone and Yun (2016)(first column) and our interpretation ("System/Series").

Description	System/Series
second fan-shaped debris flow - Holocene	Holocene
Rock-fall deposit - Holocene?	Holocene
1668 dark trachytic ignimbrite and surge - Holocene	Holocene
third fan-shaped debris flow - Holocene	Holocene
1903 phreatomagmatic eruption - Holocene	Holocene
Baitoushan III upper trachyte cone with comendite, 0.02-0.22 Ma	non-Holocene
Baithoushan II middly trachyte cone and ignimbrite, 0.25-0.44 Ma	non-Holocene

Table S27: Summary of the area calculation for Tianchi Lake.

Area Holocene (km^2)	Area non-Holocene (km^2)	Area Quaternary (km^2)	Total Area (km^2)	Holocene (%)
7.39	3.92	0	11.31	65.34

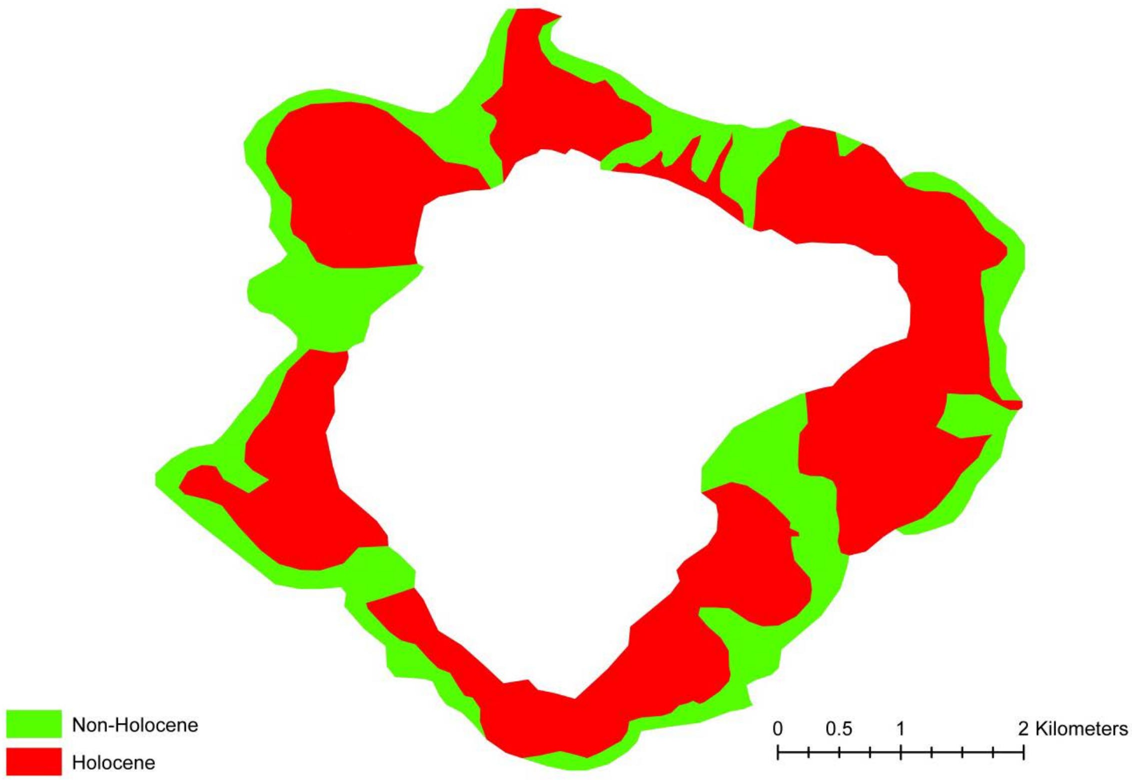

Figure S13: Map of Tianchi Lake and its surrounding lithology showing the distribution of the age of basaltic rocks.

Part Two: Additional information on relations among studied parameters

In addition to results provided in the main text further relationships among applied parameters are shown.

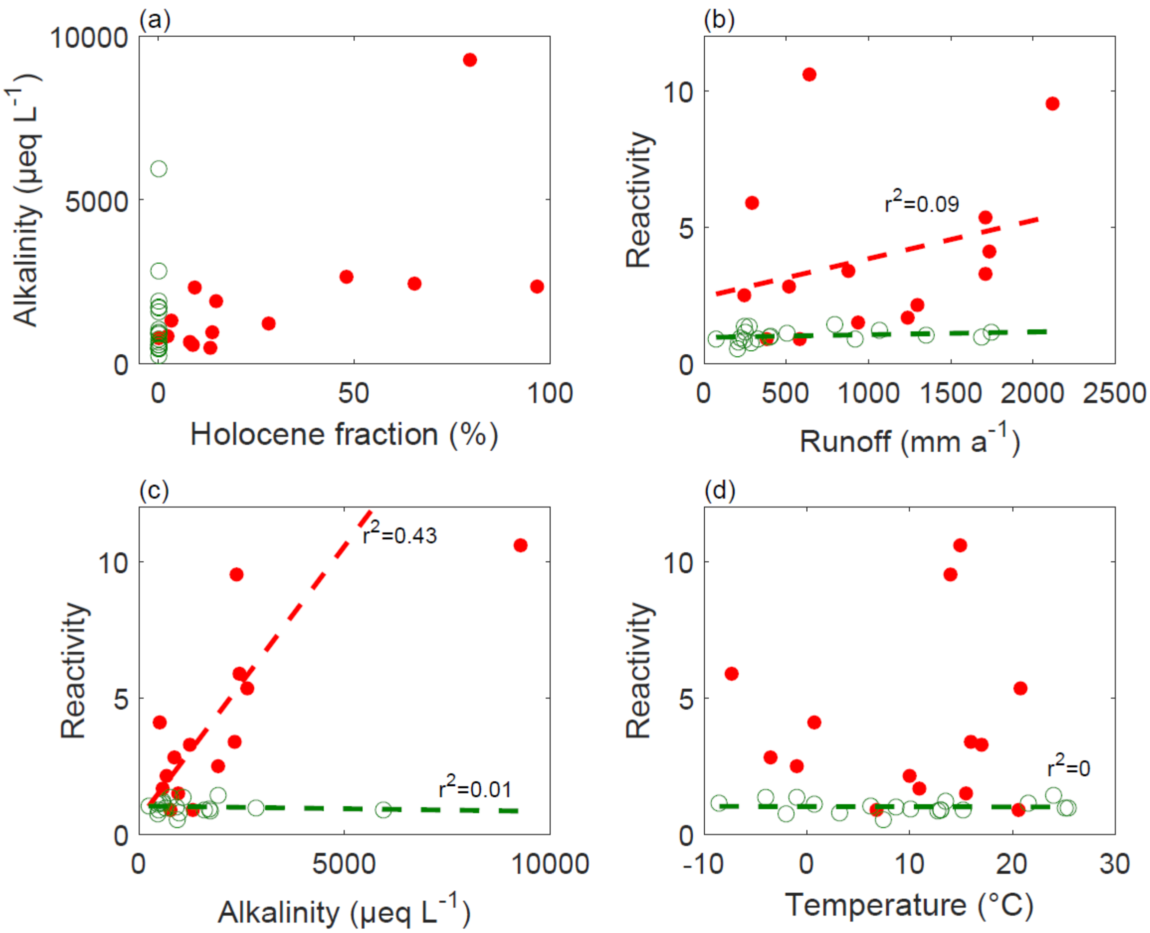

Figure 14S: Scatterplot relationships between alkalinity, Holocene fraction, reactivity and temperature. a) Holocene fraction versus alkalinity concentrations. Green: IVFs, red: AVFs. b) Reactivity versus runoff: The green regression line (IVFs) suggests almost no correlation of reactivity with runoff, also for the AVFs no significant correlation is identified (coefficient of determination r^2=0.09 and slope of 0.001 with reactivity units per mm runoff a^{-1}; excluding Mt. Etna and Mt. Cameroon). c) Reactivity versus alkalinity concentration: Excluding Mt. Etna, a coefficient of determination r^2 = 0.43 exists, suggesting an increase in reactivity due to elevated alkalinity concentration for AVFs. d) Reactivity versus temperature suggests no bias of reactivity due to a temperature effect for AVFs, as reactivity is based on a temperature normalized parameterization. For the IVFs (r^2=0) no bias with temperature can be identified due to the good correlation of alkalinity fluxes with land surface temperature (green line).

Table S28: Statistical calculations for the previous linear regression with standard deviations of the parameters. The absolute difference Dr is calculated by: CO_2 consumption$_{observed}$ – CO_2 consumption$_{predicted}$ and the slope x_i-x_{mean} is derived by: Holocene fraction – average Holocene fraction.

No.	Name	Volcanic activity	CO_2 consumption [10^6 mol/km^2/a]		Residuals		Slope	
			observed	predicted	D_r	D_r^2	x_i-x_{mean}	$(x_i-x_{mean})^2$
1	Massif Central	Inactive	0.372	0.366	0.005	0.000	-11.849	140.401
2	South Africa	Inactive	0.420	0.483	-0.063	0.004	-11.849	140.401
3	Karelia	Inactive	0.131	0.175	-0.044	0.002	-11.849	140.401
4	Coastal Deccan	Inactive	1.110	1.140	-0.030	0.001	-11.849	140.401
5	Interior Deccan	Inactive	1.138	1.164	-0.025	0.001	-11.849	140.401
6	Siberia Traps	Inactive	0.127	0.111	0.016	0.000	-11.849	140.401
7	E'Mei	Inactive	0.321	0.308	0.012	0.000	-11.849	140.401
8	Lei-Qiong	Inactive	1.532	1.056	0.475	0.226	-11.849	140.401
9	Nanjing	Inactive	0.526	0.575	-0.048	0.002	-11.849	140.401
10	Xiaoxinganling	Inactive	0.259	0.187	0.072	0.005	-11.849	140.401
11	Tumen River	Inactive	0.208	0.152	0.056	0.003	-11.849	140.401
12	Mudan River	Inactive	0.204	0.250	-0.046	0.002	-11.849	140.401
13	SE Australia	Inactive	0.441	0.493	-0.053	0.003	-11.849	140.401
14	Tasmania	Inactive	0.377	0.404	-0.027	0.001	-11.849	140.401
15	North Island	Inactive	0.439	0.493	-0.054	0.003	-11.849	140.401
16	Kauai, Hawaii	Inactive	1.026	0.894	0.133	0.018	-11.849	140.401
17	Columbia Plateau	Inactive	0.189	0.335	-0.146	0.021	-11.849	140.401
18	NE America	Inactive	0.235	0.211	0.025	0.001	-11.849	140.401
19	Madeira Island	Inactive	0.618	0.511	0.107	0.011	-11.849	140.401
20	Easter Island	Active	0.757	1.104	-0.347	0.120	-8.489	72.065
21	Mt. Cameroon	Active	5.020	5.431	-0.411	0.169	84.714	7176.452
22	Mt. Etna	Active	5.943	4.861	1.082	1.170	67.711	4584.767
23	Virunga	Active	4.522	4.749	-0.227	0.052	36.171	1308.335
24	La Réunion	Active	2.127	2.408	-0.282	0.079	16.281	265.068
25	Wudalianchi Lake	Active	0.466	0.454	0.013	0.000	2.971	8.826
26	Japan	Active	0.722	0.788	-0.066	0.004	-3.149	9.917
27	Kamchatka	Active	0.444	0.192	0.252	0.064	-9.569	91.568
28	Taranaki	Active	0.864	0.709	0.156	0.024	-3.849	14.816
29	Big Island, Hawaii	Active	0.889	1.354	-0.466	0.217	1.881	3.538
30	High Cascades	Active	0.296	0.328	-0.031	0.001	-11.649	135.701
31	São Miguel	Active	2.047	1.152	0.895	0.801	-2.499	6.245
32	Iceland	Active	0.864	0.477	0.386	0.149	1.341	1.798
33	Tianchi Lake	Active	0.711	0.881	-0.169	0.029	53.491	2861.277
	variance					0.096		0.000
	standard deviation					0.311		0.002

Part Three: Description of the global calculations

For the global calculations of alkalinity fluxes, temperature data from Hijmans et al. (2005) and runoff data from Fekete et al. (2002) were used, as well as a global basalt map, mostly based on the GLiM (Fig. S15) distinguishing areas considering Holocene area fractions for the calculations (Cenozoic) and non-Cenozoic basaltic areas.

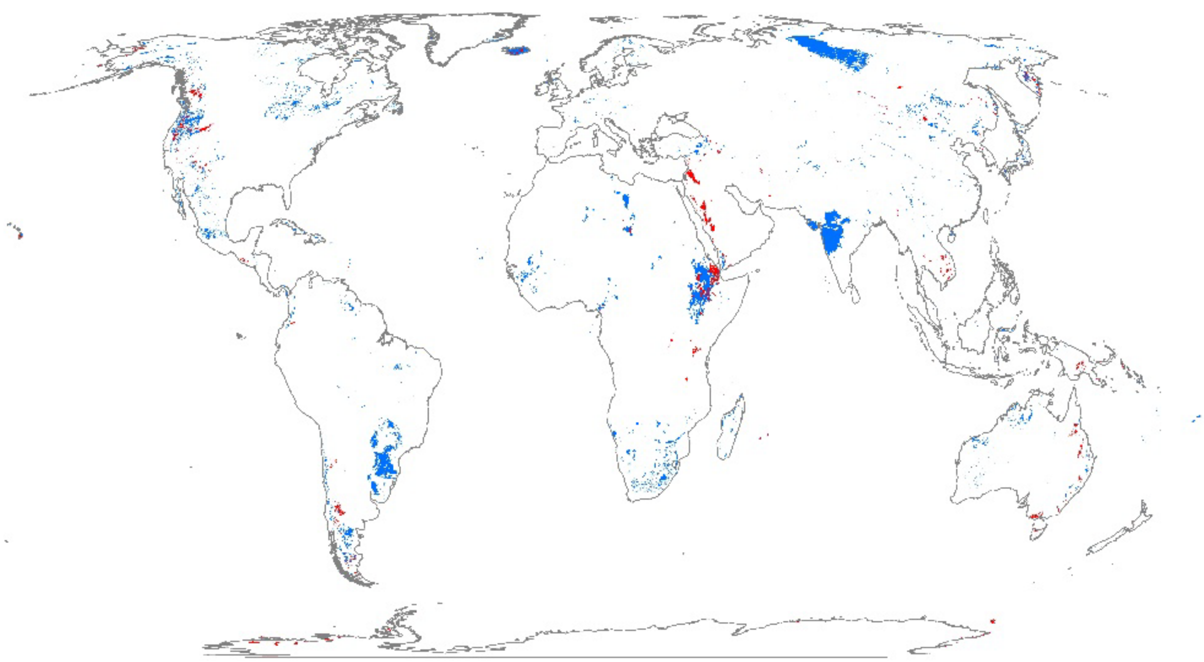

Figure S15: Global distribution of basalt areas distinguishing Cenozoic (red) and Non-Cenozoic areas (blue). The reported Holocene fractions of the Cenozoic areas are considered in the global calculation. Some areas with missing age information may result in a smaller global Holocene area fraction than applied for global calculations.

Table S29: Global calculations of CO_2 consumption for areas with a runoff >74mm/a. As reference previous global empirical equations (Bluth and Kump, 1994; Dessert et al., 2003; Goll et al., 2014; Suchet and Probst, 1995)were used to derive CO_2 consumption values.

				CO_2 consumption [10^6 mol/a]						
	Total Area [km^2]	Holocene Area [km^2]	% of global basalt area	Goll et al., 2014	Dessert et al., 2003	Amiotte-Suchet & Probst, 1995	Bluth & Kump, 1994	New equation	Area [km^2] for q>74mm/a	Holocene area [km^2] for q>74mm/a
Fluxes from purely Holocene areas	55,949	55,949	1.05	17,138	19,388	15,511	11,512	115,206	33,785	33,785
Raster with Holocene influence (Cenozoic)	932,137	55,949	17.46	233,458	247,648	118,919	93,678	314,148	359,190	33,785
Raster without Holocene influence (Non-Cenozoic)	4,406,263	-	82.54	1,237,066	1,319,226	719,451	645,354	1,677,456	3,032,768	-
TOTAL	5,338,400	55,949	100.00	1,470,525	1,566,874	838,371	739,032	1,991,604	3,391,958	33,785

Table S30: Global calculations without runoff restriction.

				CO_2 consumption [10^6 mol/a]				
	Total Area [km^2]	Holocene Area [km^2]	% of global basalt area	Goll et al., 2014	Dessert et al., 2003	Amiotte-Suchet & Probst, 1995	Bluth & Kump, 1994	New equation
Fluxes from purely Holocene areas	55,949	55,949	1.05	17,227	19,484	15,564	11,701	249,201
Raster with Holocene influence (Cenozoic)	932,137	55,949	17.46	234,714	249,063	119,831	96,017	805,917
Raster without Holocene influence (Non-Cenozoic)	4,406,263	-	82.54	1,241,945	1,324,164	722,929	657,897	2,625,217
TOTAL	5,338,400	55,949	100.00	1,476,659	1,573,227	842,760	753,915	3,431,134

A new global basalt map was derived by the combination of several different input datasets. Main input is from the Global Lithological Map (GLiM) (Hartmann and Moosdorf, 2012) whereas new data comes from geological maps that were considered for the development of the Global Unconsolidated Sediments Map (GUM) (Börker et al., 2018) and the individual active volcanoes described in this study. For the individual calculation of Holocene percentages see following tables.

Table S29: Table showing the Ages of the basaltic fields of the GLiM with the authors interpretation (third column).

Age_Min	Age_Max	HoloceneArea
Early Pleistocene	Early Pleistocene	0
Himalayan Pleistocene	Himalayan Pleistocene	0
Late Miocene to Pleistocene	Late Miocene to Pleistocene	0
Late Pleistocene	Late Pleistocene	0
Late Pliocene, Early Pleistocene, 3.3 -	Late Pliocene, Early Pleistocene, 3.3 -	0
Lower Quaternary	Lower Quaternary	0
Lower Quaternary	Miocene	0
Middle Pleistocene	Middle Pleistocene	0
Middle Quarernary	Middle Quarernary	0
Miocene to Pleistocene	Miocene to Pleistocene	0
Mostly Pleistocene	Mostly Pleistocene	0
Neogene	Paleogene	0
Neogene	Neogene	0
Paleogene to Neogene	Paleogene to Neogene	0
Pleistocene	Pliocene	0
Pleistocene	Pleistocene	0
Pleistocene	Late Miocene	0
Pleistocene and Neocene	Pleistocene and Neocene	0
Pliocene to Pleistocene	Pliocene to Pleistocene	0
Quartär, Pleistozän	Quartär, Pleistozän	0
Quaternary (0.15 Ma)	Pleistocene (0.15 Ma)	0
Quaternary (0.23 Ma)	Pleistocene (0.23 Ma)	0
Quaternary (0.26Ma)	Quaternary (0.26Ma)	0
Quaternary (0.37 Ma)	Pleistocene (0.37 Ma)	0
Quaternary (0.64-0.7Ma)	Quaternary (0.64-0.7Ma)	0
Quaternary (0.89 Ma)	Pleistocene (0.89 Ma)	0
Quaternary (1.1 Ma)	Quaternary (1.1 Ma)	0
Quaternary (1.29 Ma)	Quaternary (1.29 Ma)	0
Quaternary, >0.2Ma	Pleistocene, >0.2Ma	0
Cainozoic	Cainozoic	0.02
Cenozoic	Cenozoic	0.02
Quaternary	Tertiary	0.02
Quaternary	Cainozoic	0.02

Quaternary and Tertiary	Quaternary and Tertiary	0.02
QUATERNARY OR TERTIARY	QUATERNARY OR TERTIARY	0.02
Tertiary(?) and Quaternary	Tertiary(?) and Quaternary	0.02
Tertiary-Quaternary	Tertiary-Quaternary	0.02
Oligocene and younger	Oligocene and younger	0.03
Holocene	Miocene	0.05
Miocene to Holocene	Miocene to Holocene	0.05
Miocene to Quaternary	Miocene to Quaternary	0.05
Neogene	Quaternary	0.05
Neogene to Holocene	Neogene to Holocene	0.05
quaternary	neogene	0.05
Quaternary	Neogene	0.05
PLIOCENO-PLEISTOCENO-HOLOCENO	PLIOCENO-PLEISTOCENO-HOLOCENO	0.22
Quaternary	Pliocene	0.22
Quaternary to Pliocene	Quaternary to Pliocene	0.22
Quaternary (0-4 Ma)	Quaternary (0-4 Ma)	0.29
Middle Pliocene to Holocene	Middle Pliocene to Holocene	0.33
Holocene	Pleistocene	0.45
Pleistocene to Holocene	Pleistocene to Holocene	0.45
Quaternary	Upper Quaternary	0.45
Quaternary	Pleistocene	0.45
Quaternary	Quaternary	0.45
Upper Quaternary	Middle Quarernary	0.45
Quaternary, <0.4Ma	Pleistocene, <0.4Ma	2.93
Quaternary (<0.27 Ma)	Pleistocene (<0.27 Ma)	4.33
Late Pleistocene to Holocene	Late Pleistocene to Holocene	9.29
Quaternary (ca. 10-20 000 yrs BP)	Quaternary (ca. 10-20 000 yrs BP)	17
Holocene, <40ka	Holocene, <40ka	29.25
Holocene	Holocene	100
Holocene (postglacial time)	Holocene (postglacial time)	100
Upper Quaternary	Upper Quaternary	100

Table S30: Table showing the age classifications of additional data of several geological maps that were used for the GUM database with our interpretation (third column). Map sources are: Afghanistan (Doebrich et al., 2006), Australia (Raymond et al., 2012), Austria (Geologische Bundesanstalt (GBA), 2013), Bolivia (GeoBolivia, 2000), Canada (Fulton, 1995), Caribbean region (French and Schenk, 2004), China (China Geological Survey, 2002), Colombia (Gomez Tapias et al., 2015), Ethiopia (Tefera et al., 1996), Iran (Pollastro et al., 1999), Japan (Geological Survey of Japan AIST (ed.) (2009), https://gbank.gsj.jp/seamless/download/downloadIndex_e.html, accessed May 2016), North Africa 1 (Alimen et al., 1973), North Africa 2 (Alimen et al., 1978), Russia (Zastrozhnov et al., 2014), Siegen, Trier, Köln, Frankfurt (Main, west) (Bundesanstalt für Geowissenschaften und Rohstoffe, 2007), Spain (Canaries Islands), Spain (Instituto Geológico y Minero de España, 1988), Tanzania (Geological Survey of Tanzania, Geo-Economic Data (1:2M) – Geology, http://www.gmis-tanzania.com/, accessed May 2016), USA (Soller et al., 2009).

Age_Min	Age_Max	HoloceneArea
0.19M	0.215M	0
0.45M	0.65M	0
Plio/Pleistocene	Sarmatian/Pannonian	0
Pleistocene	Pliocene	0
0.26M	1M	0
0.3M	1M	0
0.01M	2.5M	0
Early Pleistocene	Early Pleistocene	0
0.126	0.780	0
Middle Pleistocene	Middle Pleistocene	0
Late Pleistocene	Late Pleistocene	0
Pleistocene	Pleistocene	0
Middle Pleistocene	Late Pleistocene	0
Early Pleistocene	Middle Pleistocene	0
Cenozoic	Cenozoic	0.02
0	23Ma	0.05
Holocene	Pliocene	0.22
Quaternary	Quaternary	0.45
Holocene	Late Pleistocene	9.29

References

Alimen, H., Choubert, G., International association for quaternary research, Unesco, 1973. Carte Internationale du Quaternaire de l'Afrique 1:2,500,000 - Afrique du nord / Prepared by the Subcommission of INQUA for the Quaternary map of Africa under the aegis of the National Centre of Scientific Research. United Nations Educational, Scientific and Cultural Organization, Sub-Commission of INQUA for the *Quaternary Map of Africa*, Paris.

Alimen, H., Choubert, G., International association for quaternary research, Unesco, 1978. Carte Internationale du Quaternaire de l'Afrique 1:2,500,000 - Sahara Occidental / Prepared by the Subcommission of INQUA for the Quaternary map of Africa with the support of the National Centre of Scientific Research. United Nations Educational, Scientific and Cultural Organization, Sub-Commission of INQUA for the *Quaternary Map of Africa*, Paris.

Balagizi, C.M. et al., 2015. River geochemistry, chemical weathering, and atmospheric CO2 consumption rates in the Virunga Volcanic Province (East Africa). Geochemistry, Geophysics, Geosystems, 16(8): 2637-2660.

Bluth, G.J., Kump, L.R., 1994. Lithologic and climatologic controls of river chemistry. Geochimica et Cosmochimica Acta, 58(10): 2341-2359.

Börker, J., Hartmann, J., Amann, T., Romero-Mujalli, G., 2018. Terrestrial sediments of the earth: development of a global unconsolidated sediments map database (GUM). Geochemistry, Geophysics, Geosystems, 19.

Branca, S., Coltelli, M., Groppelli, G., Lentini, F., 2011. Geological map of Etna volcano, 1: 50,000 scale. Italian Journal of Geosciences, 130(3): 265-291.

Bundesanstalt für Geowissenschaften und Rohstoffe, 2007. Geologische Übersichtskarte der Bundesrepublik Deutschland 1:200,000 (GÜK200).

China Geological Survey, 2002. Geological Atlas of China - Chinese geological map (1:2,500,000). Geological Press.

De Mulder, M., Hertogen, J., Deutsch, S., André, L., 1986. The role of crustal contamination in the potassic suite of the Karisimbi volcano (Virunga, African Rift Valley). Chemical geology, 57(1): 117-136.

Dessert, C., Dupré, B., Gaillardet, J., François, L.M., Allègre, C.J., 2003. Basalt weathering laws and the impact of basalt weathering on the global carbon cycle. Chemical Geology, 202(3–4): 257-273.

Doebrich, J.L. et al., 2006. Geologic age and lithology of Afghanistan (glgafg.shp), U.S. Geological Survey Open File Report. U.S. Geological Survey, Denver, CO. U.S.A.

Fekete, B.M., Vörösmarty, C.J., Grabs, W., 2002. High-resolution fields of global runoff combining observed river discharge and simulated water balances. Global Biogeochemical Cycles, 16(3).

French, C.D., Schenk, C.J., 2004. Surface Geology of the Caribbean Region (geo6bg). U.S. Geological Survey, Central Energy Resources Team, Denver, Colorado.

Fulton, R., 1995. Surficial materials of Canada. In: Geological Survey of Canada (Editor), Map 1880A, scale 1:5 000 000. Natural Resources Canada, Ottawa.

GeoBolivia, 2000. Mapa geologico de Bolivia, 2000. Servicio Nacional de Geología y Técnico de Minas - SERGEOTECMIN.

Geological Survey of Japan AIST (ed.), 2009. Seamless digital geological map of Japan 1:200,000. Dec 15, 2009 version. Research Information Database DB084. Geological Survey of Japan, National Institute of Advanced Industrial Science and Technology.

Geologische Bundesanstalt (GBA), 2013. Kartographisches Modell 1:500000 Austria - Geologie.

Gioncada, A. et al., 2010. The volcanic rocks of Easter Island (Chile) and their use for the Moai sculptures. European Journal of Mineralogy, 22(6): 855-867.
Goll, D.S., Moosdorf, N., Hartmann, J., Brovkin, V., 2014. Climate-driven changes in chemical weathering and associated phosphorus release since 1850: Implications for the land carbon balance. Geophysical Research Letters, 41(10): 3553-3558.
Gomez Tapias, J. et al., 2015. Explanatory notes: Geological Map of Colombia. In: Gomez, J., Almanza, M.F. (Eds.), Compilando la geologia de Colombia: Una vision a 2015. Servicio Geologico Colombiano, Publicaciones Geológicas Especiales 33, Bogotá, pp. 35-60.
Hartmann, J., Moosdorf, N., 2012. The new global lithological map database GLiM: A representation of rock properties at the Earth surface. Geochemistry, Geophysics, Geosystems, 13(12).
Hijmans, R.J., Cameron, S.E., Parra, J.L., Jones, P.G., Jarvis, A., 2005. Very high resolution interpolated climate surfaces for global land areas. International journal of climatology, 25(15): 1965-1978.
Instituto Geológico y Minero de España, 1988. Mapa del Cuaternario de España a escala 1:1.000.000.
Le Maréchal, A., 1975. Carte geologique de l'ouest du Cameroun et de l'Adamaoua. ORSTOM.
Li, G. et al., 2016. Temperature dependence of basalt weathering. Earth and Planetary Science Letters, 443: 59-69.
Moore, R.B., 1990. Volcanic geology and eruption frequency, São Miguel, Azores. Bulletin of Volcanology, 52(8): 602-614.
Neall, V., Stewart, R., Smith, I., 1986. History and petrology of the Taranaki volcanoes. Royal Society of New Zealand Bulletin, 23: 251-263.
Nehlig, P., Quinquis, J., Bucelle, M., Odon, O., 2006. Carte géologique de la Réunion. Bur. de Rech. Geol. et Min., Orleans, France.
Paone, A., Yun, S.-H., 2016. Pyroclastic Density Current Hazards at the Baekdusan Volcano, Korea: Analyses of Several Scenarios from a Small-Case to the Worst-Case Colossal Eruption, Updates in Volcanology-From Volcano Modelling to Volcano Geology. InTech.
Petricec, V., Gerards, J., Antun, P., 1971. Carte Géologique du Rwanda, Feuille Ruhengeri Nord (S2/29 NW et NE), Champs Volcanique des Birunga. Institut Géographique Militaire de Belgique.
Pollastro, R.M., Persits, F., Steinshouer, D., 1999. Surficial geology of Iran (geo2cg). U.S. Geological Survey, Central Energy Ressources Team.
Price, R., McCulloch, M., Smith, I., Stewart, R., 1992. Pb-Nd-Sr isotopic compositions and trace element characteristics of young volcanic rocks from Egmont Volcano and comparisons with basalts and andesites from the Taupo Volcanic Zone, New Zealand. Geochimica et cosmochimica acta, 56(3): 941-953.
Raymond, O.L., Liu, S., Gallagher, R., Highet, L.M., Zhang, W., 2012. Surface Geology of Australia, 1:1 million scale, dataset 2012 edition. Commonwealth of Australia (Geoscience Australia).
Smets, B., Wauthier, C., d'Oreye, N., 2010. A new map of the lava flow field of Nyamulagira (DR Congo) from satellite imagery. Journal of African Earth Sciences, 58(5): 778-786.
Soller, D.R., Reheis, M.C., Garrity, C.P., Van Sistine, D.R., 2009. Map database for surficial materials in the conterminous United States. US Geological Survey Data Series, 425.
Stearns, H.T., Macdonald, G.A., 1946. Geology and ground-water resources of the island of Hawaii, Honolulu Advertising.
Suchet, P.A., Probst, J.L., 1995. A global model for present-day atmospheric/soil CO2 consumption by chemical erosion of continental rocks (GEM-CO2). Tellus B, 47(1-2): 273-280.
Tefera, M., Chernet, T., Haro, W., 1996. Geological Map of Ethiopia. Ministry of Mines, Geological Survey of Ethiopia, GSE.

Zastrozhnov, A.S. et al., 2014. Map of the Quaternary Formations of the Russian Federation. Ministry of Natural Resources and Ecology of the Russian Federation, Federal Agency on Mineral Resources, Federal State Unitary Enterprise "A.P. Karpinsky Russian Geological Research Institute" (VSEGEI), Federal State Unitary Enterprise "I.S. Gramberg Russian Research Institute for Geology and Mineral Resources of the Ocean" (VNIIOkeangeologia).